

PACS numbers: 42.81.Dp; 42.70.Qs
DOI: 10.1070/QE2006v036n01ABEH013104

Numerical simulation of photonic-crystal tellurite-tungstate glass fibres used in parametric fibre devices

V.O. Sokolov, V.G. Plotnichenko, V.O. Nazaryants, E.M. Dianov

Abstract. **Using the MIT Photonic-Bands Package to calculate fully vectorial definite-mode eigenmodes of Maxwell's equations with periodic boundary conditions in a plane-wave basis, light propagation is simulated in fibres formed by point defects in two-dimensional periodic lattices of cylindrical holes in a glass or of glass tubes. The holes and gaps between tubes are assumed filled with air. Single-site hexagonal and square lattices are considered, which were most often studied both theoretically and experimentally and are used to fabricate silica photonic-crystal fibres. As a defect, a single vacancy is studied – the absent lattice site (one hole in a glass or one of the tubes are filled with the same glass) and a similar vacancy with nearest neighbours representing holes of a larger diameter. The obtained solutions are analysed by the method of effective mode area. The dependences of the effective refractive index and dispersion of the fundamental mode on the geometrical parameters of a fibre are found. The calculations are performed for tellurite-tungstate $80TeO_2 - 20WO_3$ glass fibres taking into account the frequency dispersion of the refractive index.**

Keywords: *tellurite-tungstate glass, optical fibre, photonic crystals.*

In this paper, we considered fibres representing a fragment of a two-dimensional photonic crystal with a spatially periodic dependence of the refractive index in the cross section and a defect in the central region. The latter forms the fibre core, while the surrounding lattice forms the fibre cladding. We will call such fibres photonic-crystal fibres (PCFs).

It is known that due to a cladding in the form of a photonic crystal, PCFs possess a number of properties different from those of usual fibres. For example, PCFs can be single-mode in a very broad wavelength range [1]. The magnitude and slope of dispersion can change strongly depending on the geometrical parameters of PCFs, which allows one, for example, to shift its zero value to considerably shorter wavelengths compared to a glass, and to obtain dispersion with a small slope in a rather broad wavelength range or the required dispersion at a given wavelength [2 – 5]. Scaling of the geometry of a single-mode PCF makes it possible to change the effective mode area in a broad range (almost by two orders of magnitude), which provides the control of the magnitude of nonlinear effects in PCFs [4, 6].

Currently PCFs based on a silica glass v-SiO_2 are being actively fabricated and studied (see, for example [7, 8]). However, materials with higher values of the refractive index and nonlinear susceptibilities than for v-SiO_2 are required for many applications. Glasses based on TeO_2 (see, for example, [9, 10]) belong to such materials and are now successfully used to fabricate PCFs [11, 12].

The main task of our paper is the search for PCF structures based on a tellurite glass, which can be used in fibre parametric devices (amplifiers, etc.) operating at a wavelength of 1.55 μm. The basic requirements to such PCFs are:

(i) the high third-order susceptibility;

(ii) the possibility of obtaining a sufficiently high power density in a fibre core, i.e., a sufficiently small core diameter;

(iii) the zero efficient dispersion near the operating wavelength;

(iv) the single-mode operation.

We simulated numerically the propagation of light in fibres representing a point defect in a two-dimensional periodic lattice formed by either cylindrical holes in a glass or by glass tubes with holes and gaps between them filled with air ($\varepsilon = 1$). We considered single-site hexagonal and square lattices, which were most often studied theoretically and experimentally and are used for fabricating silica PCFs. As a defect, we studied a single vacancy – the absent lattice site (one hole in a glass or one tube filled with the same glass) and a similar vacancy with nearest neighbours representing holes of a larger diameter. Figures 1 – 4 show fragments of the corresponding lattices in the defect vicinity. We used the following notation of PCFs studied in the paper:

HH PCF: a PCF formed by a filled central hole in a simple hexagonal lattice of cylindrical holes in a glass;

SH PCF: a PCF formed by a filled central hole in a simple square lattice of cylindrical holes in a glass;

HH1 PCF: a PCF formed by a filled central hole in a simple hexagonal lattice of cylindrical holes in a glass and by the larger-diameter holes of the first row around the filled hole;

V.O. Sokolov, V.G. Plotnichenko, V.O. Nazaryants, E.M. Dianov Fiber Optics Research Center, A.M. Prokhorov General Physics Institute, Russian Academy of Sciences, ul. Vavilova 38, 119991 Moscow, Russia; e-mail: sokolov@fo.gpi.ac.ru, victor@fo.gpi.ac.ru

Received 13 October 2005
Kvantovaya Elektronika **36** (1) 67 – 72 (2006)
Translated by M.N. Sapozhnikov

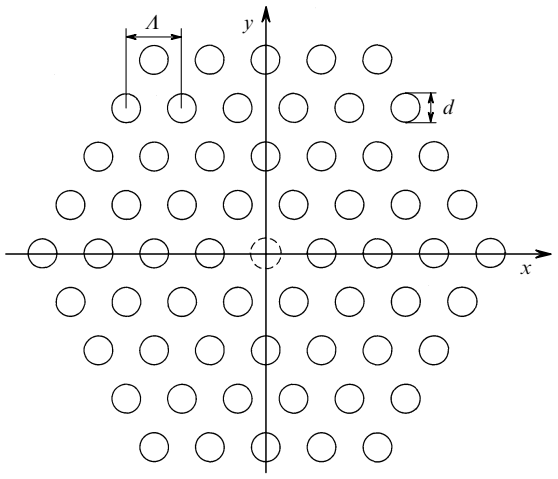

Figure 1. Fragment of a hexagonal lattice of holes in a glass (HH PCF). The dashed circle shows the absent hole representing a defect (vacancy) in the regular lattice of holes.

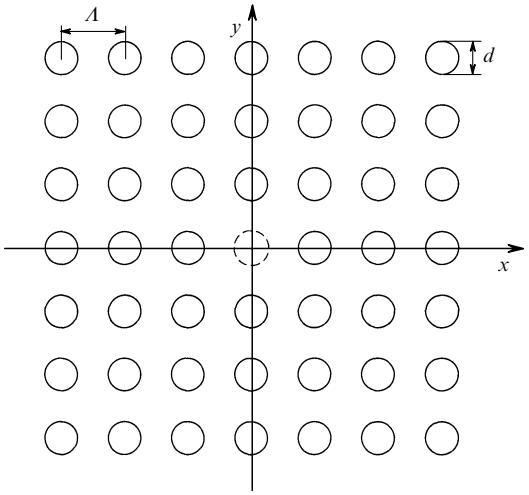

Figure 2. Fragment of a square lattice of holes in a glass (SH PCF). The dashed circle shows the absent hole representing a defect (vacancy) in the regular lattice of holes.

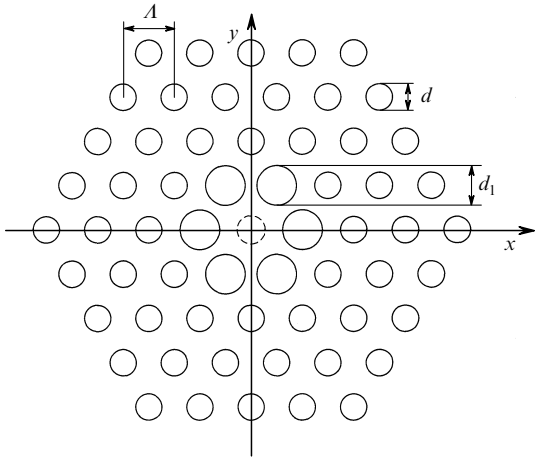

Figure 3. Fragment of a hexagonal lattice of holes in a glass with a vacancy surrounded by larger-diameter holes (HH1 PCF). The dashed circle shows the absent hole in a central tube representing a defect (vacancy) in the regular lattice of holes.

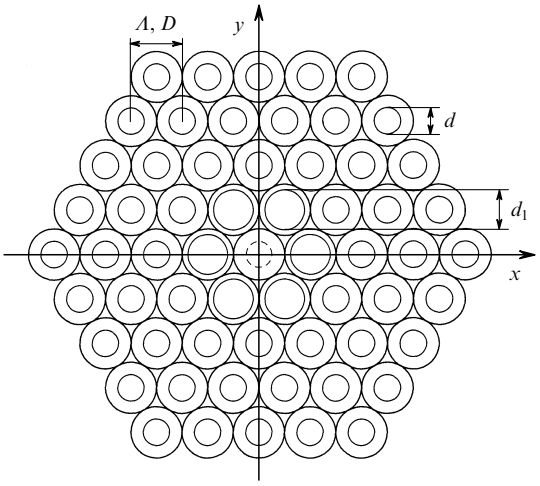

Figure 4. Fragment of a hexagonal lattice of glass tubes with a vacancy surrounded by tubes with the larger internal diameter (HT1 PCF). The dashed circle shows the absent hole in a central tube (vacancy).

HT1 PCF: a PCF formed by a filled tube in a simple hexagonal lattice of cylindrical glass tubes and by tubes with a larger inner diameter in the first row around the filled tube.

All the calculations were performed for tellurite-tungstate $80TeO_2 - 20WO_3$ (below, simply tellurite) glass fibres taking into account the frequency dispersion of its permittivity. The experimental dependence of the latter in the transparency region of the glass was approximated by the Sellmeyer formula

$$\varepsilon(\lambda) = A + B(1 - C\lambda^{-2})^{-1} + D(1 - E\lambda^{-2})^{-1},$$

where the coefficients $A = 2.4909866$, $B = 1.9515037$, $C = 5.6740339 \times 10^{-2}$ μm^2, $D = 3.0212592$, and $E = 225$ μm^2 are taken from [13] and the wavelength λ is measured in μm.

Below, we used the following notation: Λ is the lattice period, which is obviously equal to the external diameter D of a tube for a lattice made of tubes; d is the diameter of holes in a glass or the internal diameter of a tube; d_1 is the diameter of holes in a glass (the internal diameter of tubes) of the first row around the vacancy (if it differs from d); ε is the glass permittivity; λ is the wavelength of the incident light in vacuum; ω is the light frequency; c is the speed of light in vacuum; β is the propagation constant of the fibre; $\boldsymbol{k}$ is the wave vector; and $A_{\text{eff}}^{(i)}$ is the effective area of the ith mode. We assume that light propagates along the z axis (perpendicular to the xy lattice plane).

According to [14], the effective mode area is

$$A_{\text{eff}}^{(i)} = \frac{\left[\int I^{(i)}(\boldsymbol{r}_\perp)\mathrm{d}^2 r_\perp\right]^2}{\int[I^{(i)}(\boldsymbol{r}_\perp)]^2\mathrm{d}^2 r_\perp},$$

where $\boldsymbol{r}_\perp$ are coordinates in the xy lattice plane and $I^{(i)}(\boldsymbol{r}_\perp)$ is the intensity of the ith mode.

The numerical aperture NA was defined according to [15] as $\mathrm{NA} = \sin\vartheta$, where ϑ is the half-angle of the beam divergence. The numerical aperture is related to the effective mode area by the expression [15]

$$\mathrm{NA} \approx \left(1 + \pi\frac{A_{\text{eff}}}{\lambda^2}\right)^{-1/2}.$$

The effective refractive index is

$$n_{\text{eff}} = \beta \frac{c}{\omega},$$

and the effective dispersion is

$$M = -\frac{\lambda}{c} \frac{\mathrm{d}^2 n_{\text{eff}}(\lambda)}{\mathrm{d}\lambda^2}.$$

All the calculations were performed by using the MIT Photonic-Bands package [16] (below, MPB), which allows one to find vector eigenfunctions of Maxwell's equations with periodic boundary conditions in the plane-wave basis. The details of numerical calculations, the features of their realisation in the MPB package and the operation with the package are described in [16, 17].

A PCF representing a point defect in a two-dimensional periodic lattice was calculated by the expanded cell method [17]. We used in our calculations a cell of size 12×12 lattice periods with a vacancy at its centre. The calculations were performed for the centre of the Brillouin zone (point Γ) of the expanded cell. Such an approach allows one to study localised modes concentrated in the vacancy vicinity of diameter $\sim 4\Lambda$, which are the guided modes of the PCF. Our calculations showed that for all localised modes described below the diameter of the localisation region is noticeably smaller than 4Λ, i.e., the periodic boundary conditions for the expanded cell almost do not affect the character of these solutions.

PCFs of each type were calculated for four lattice periods changing in the range $1\ \mu\text{m} \lesssim \Lambda \lesssim 3\ \mu\text{m}$, and for each period – for the relative diameters of holes (internal diameters of tubes) equal to $d/\Lambda = 0.2$, 0.4, 0.6, and 0.8. In the case of the HH1 and HT1 fibres, calculations were also performed for the relative diameters of the first-row holes $d_1/\Lambda = 0.6$, 0.7, and 0.8. For each set of geometrical parameters, we calculated the effective refractive index for the fundamental (first) mode of the PCF, its effective dispersion, the effective area of the three lowest modes of the PCF (each of them being doubly degenerate in polarisation), and the numerical aperture for the fundamental mode. Based on these data, we selected the values of geometrical parameters satisfying all the above-mentioned requirements imposed on the PCFs for parametric devices, and selected in this way several PCFs whose properties will be discussed below. For each of the selected PCFs we performed additional calculations with geometrical parameters differing from the optimal ones by $\pm 5\,\%$ in order to verify the stability of the PCF properties to the possible scatter in these parameters during fibre fabrication. All the calculations were performed for the same set of wavelength in the range from 1.0 to 2.4 μm.

HH PCF with the lattice period $\Lambda = 1.50$ μm. Figure 5 shows the wavelength dependences of the effective dispersion M for the fundamental mode for several values of the relative hole diameter. One can see that for $d = 0.52\Lambda = 0.78$ μm, this PCF has the zero effective dispersion at a wavelength of 1.545 μm, the dispersion slope in the vicinity of this wavelength being ~ 0.37 ps nm^{-2} km^{-1}. The effective area of the fundamental mode at the operating wavelength 1.55 μm is $A_{\text{eff}} = 1.3096\Lambda^2 \approx 3.0\ \mu\text{m}^2$ and the numerical aperture is NA ≈ 0.60. Such a PCF is single-mode at wavelengths $\lambda \gtrsim 1.1$ μm.

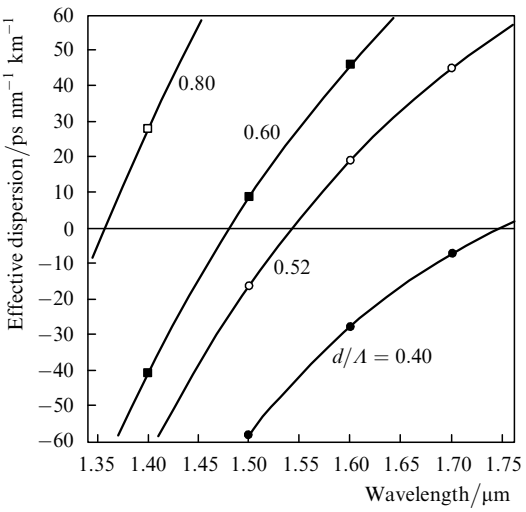

Figure 5. Spectral dependences of the effective dispersion for the fundamental mode in a hexagonal lattice of holes in a $80\text{TeO}_2 - 20\text{WO}_3$ glass ($\Lambda = 1.50$ μm) for different relative diameters d/Λ of holes.

Figure 6 shows the dependence of the effective dispersion curve on the geometrical parameters d and Λ of the PCF. One can see that as the transverse scale and diameter of the lattice holes change by $\pm 5\,\%$, the dispersion zero shifts by 10 and 15 nm, respectively, and the dispersion slope changes by ~ 0.01 ps nm^{-2} km^{-1}.

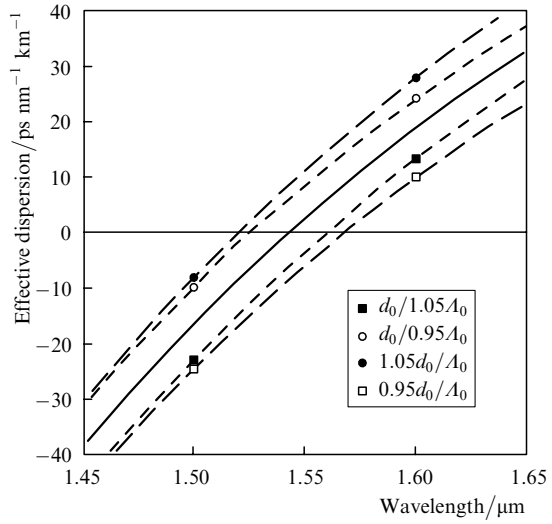

Figure 6. Influence of geometrical parameters on the effective dispersion for the fundamental mode in a hexagonal lattice of holes in a $80\text{TeO}_2 - 20\text{WO}_3$ glass (the initial values are $\Lambda_0 = 1.50$ μm and $d_0/\Lambda_0 = 0.52$). Here and in Figs 8, 10, 12, the solid curve corresponds to $\Lambda = \Lambda_0$ and $d = d_0$.

SH PCF with the lattice period $\Lambda = 1.20$ μm. One can see from the wavelength dependences of the effective dispersion for the fundamental mode shown in Fig. 7 for several values of d/Λ that for $d = 0.53\Lambda = 0.64$ μm the effective dispersion vanishes at $\lambda = 1.551$ μm and the dispersion slope in the vicinity of this wavelength is ~ 0.28 ps nm^{-2} km^{-1}. In this case, the effective area of the fundamental mode is $A_{\text{eff}} = 0.7665\Lambda^2 \approx 2.5\ \mu\text{m}^2$, the numerical aperture is NA ≈ 0.47 at the operating wavelength 1.55 μm, and the PCF is single-mode for $\lambda \gtrsim 0.9$ μm.

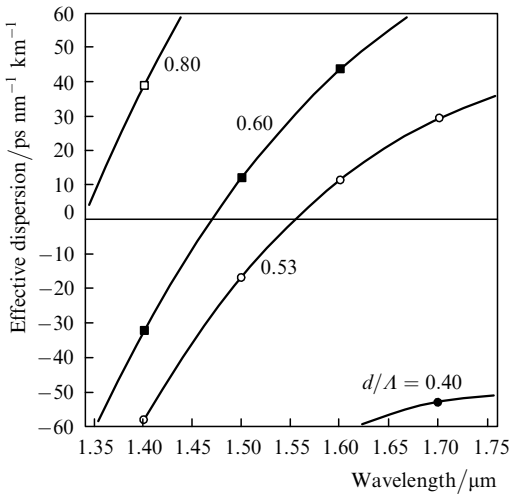

Figure 7. Spectral dependences of the effective dispersion for the fundamental mode in a square lattice of holes in a $80TeO_2 - 20WO_3$ glass ($\Lambda = 1.20$ μm) for different relative diameter d/Λ of holes.

Figure 8 shows the dependence of the effective dispersion curve on the geometrical parameters of the PCF varied by ±5 %. The change in the transverse scale results in the shift of the dispersion zero approximately by 4 nm, whereas the decrease or increase in the hole diameter by 5 % causes the shift of the dispersion zero by 40 and 50 nm, respectively. In the former case, the slope of the dispersion curve changes by ~ 0.02 ps nm^{-2} km^{-1} and in the latter by 0.05 ps nm^{-2} km^{-1}.

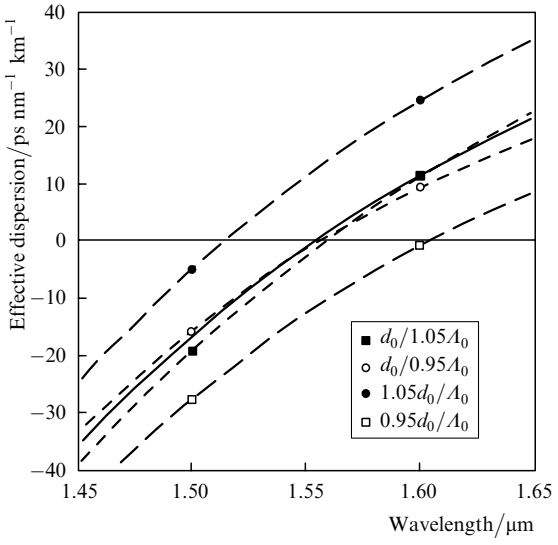

Figure 8. Influence of geometrical parameters on the effective dispersion for the fundamental mode in a square lattice of holes in a $80TeO_2 - 20WO_3$ glass (the initial values are $\Lambda = 1.20$ μm and $d_0/\Lambda_0 = 0.53$).

HH1 PCF with the lattice period $\Lambda = 2.20$ μm and the diameter of the first-row holes around the central filled hole $d_1 = 0.80\Lambda = 1.76$ μm. Our calculations showed that such structures have waveguide properties in the wavelength range under study only when other holes of the lattice have sufficiently large diameters, namely, when $d \gtrsim 0.5\Lambda = 1.1$ μm. Figure 9 shows the wavelength dependence of the effective dispersion for the fundamental mode. It follows from the calculations that in the region $d \gtrsim 0.5\Lambda$ the effective dispersion is virtually independent of the diameter of lattice holes, vanishing at a wavelength of 1.542 μm, with the slope ~ 0.40 ps nm^{-2} km^{-1}. At the operating wavelength $\lambda = 1.55$ μm, the effective area of the fundamental mode is $A_{\text{eff}} = 0.7342\Lambda^2 \approx 3.6$ μm^2 and the numerical aperture is NA ≈ 0.41. Such a PCF is single-mode at wavelengths $\lambda \gtrsim 1.1$ μm for $d \lesssim 0.7\Lambda = 1.5$ μm.

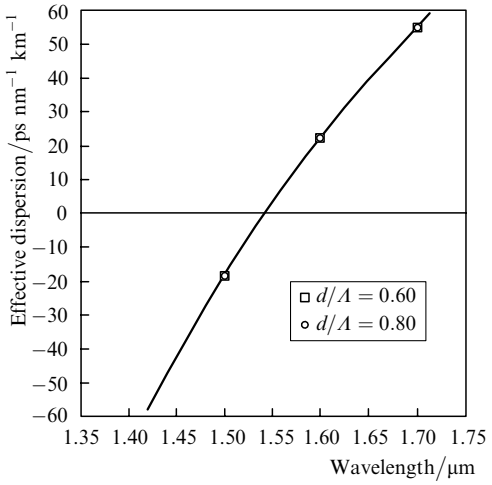

Figure 9. Spectral dependences of the effective dispersion for the fundamental mode in a hexagonal lattice of holes in a $80TeO_2 - 20WO_3$ glass with the increased diameter of the first-row holes ($\Lambda = 2.20$ μm, $d_1/\Lambda = 0.80$) for $d/\Lambda = 0.60$ and 0.80.

Figure 10 shows the dependence of the effective dispersion curve on the geometrical parameters of the PCF. As follows from the above said, a change in the relative diameter of the lattice holes d/Λ does not affect the effective dispersion, whereas changes in the transverse size and the diameter of the first-row holes around the central filled hole by ±5 % cause the shift of the dispersion zero approx-

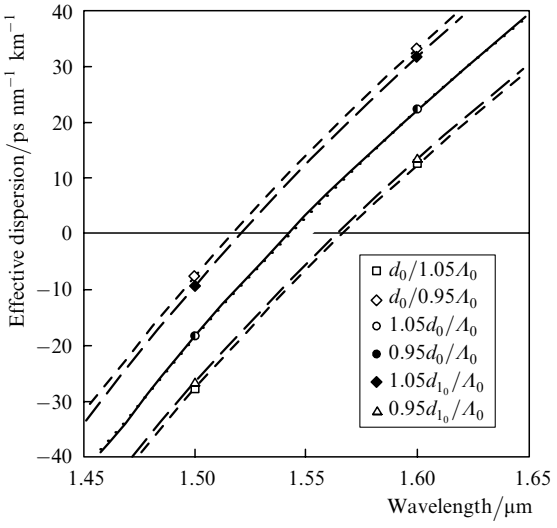

Figure 10. Influence of geometrical parameters on the effective dispersion for the fundamental mode in a hexagonal lattice of holes in a $80TeO_2 - 20WO_3$ glass with the increased diameter of the first-row holes (the initial values are $\Lambda_0 = 2.20$ μm, $d_0/\Lambda_0 = 0.60$, and $d_{1_0}/\Lambda_0 = 0.80$).

imately by 24 nm. The slope of the dispersion curve in this case changes no more than by 0.01 ps nm^{-2} km^{-1}.

HT1 PCF with the lattice period (external diameter of tubes) $\Lambda = D = 2.70$ μm and the internal diameter of the first-row tubes around the central filled tube $d_1 = 0.80\Lambda = 2.16$ μm. According to our calculations, these structures have waveguide properties in the wavelength range under study for all practically important internal diameters of the rest of the tubes forming the lattice ($d \gtrsim 0.1\Lambda \approx 0.25$ μm), the PCF being single-mode at the wavelengths $\lambda \gtrsim 0.8$ μm for $d \lesssim 0.3\Lambda \approx 0.80$ μm. The spectral dependences of the effective dispersion for the fundamental mode are shown in Fig. 11. In the region $d \gtrsim 0.1\Lambda$, the effective dispersion is almost independent of the internal diameter of tubes. The dispersion is zero at $\lambda = 1.548$ μm and the dispersion slope in the vicinity of this wavelength is 0.40 ps nm^{-2} km^{-1}. At the operating wavelength $\lambda = 1.55$ μm, the effective area of the fundamental mode is $A_{\text{eff}} = 0.4564\Lambda^2 \approx 3.3$ μm^2 and the numerical aperture is NA ≈ 0.42.

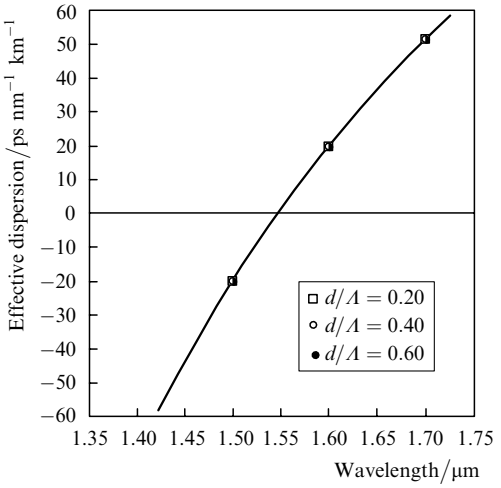

Figure 11. Spectral dependences of the effective dispersion for the fundamental mode in a hexagonal lattice of tubes in a $80TeO_2 - 20WO_3$ glass with the increased diameter of the first-row tubes ($\Lambda = 2.70$ μm, $d_1/\Lambda = 0.80$) for $d/\Lambda = 0.20$, 0.40, and 0.60.

The influence of the geometrical parameters of the PCF on the effective dispersion is shown in Fig. 12. One can see that the effective dispersion is almost independent of the relative internal diameter d/Λ of tubes forming the lattice. As the transverse scale or the internal diameter d_1 of the first-row tubes changes by ±5 %, the dispersion zero shifts by ~ 22 and 10 nm, respectively, while the slope of the dispersion curve changes in both cases by no more than 0.01 ps nm^{-2} km^{-1}.

Among all the fibres studied, the SH PCF has the smallest effective mode area, the smallest dispersion slope near the dispersion zero (approximately 25 % smaller than for the rest of PCFs), and the best stability of the dispersion curve to variations in the transverse scale (the shift of the dispersion zero is approximately five times smaller than that for the rest of PCFs). On the other hand, the SH PCF has the worst stability of the dispersion zero with respect to variations in the diameter of lattice holes (the shift of the dispersion zero is almost twice that of the rest of PCFs).

The characteristic feature of HH1 and HT1 PCFs with

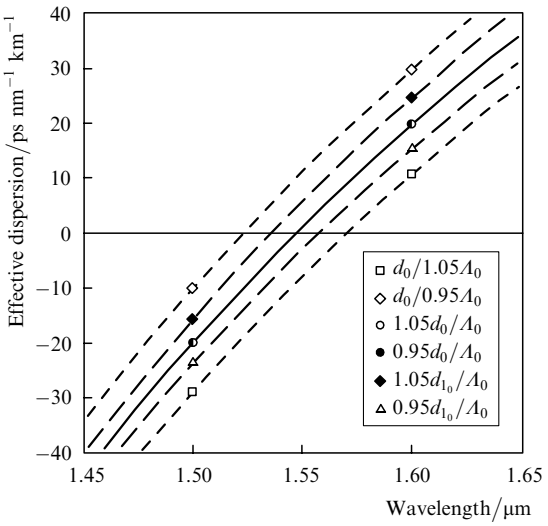

Figure 12. Influence of geometrical parameters on the effective dispersion for the fundamental mode in a hexagonal lattice of tubes in a $80TeO_2 - 20WO_3$ glass with the increased diameter of the first-row tubes (the initial values are $\Lambda_0 = 2.70$ μm, $d_0/\Lambda_0 = 0.20$, and $d_{1_0}/\Lambda_0 = 0.80$).

increased diameters d_1 of the first-row holes is the virtual absence of the influence of the diameter d of holes of the rest of the lattice on the dispersion curve (see Figs 9 and 11). However, because the diameter d determines the number of guided modes, HH1 and HT1 PCFs are single-mode only when this diameter is sufficiently small. The stability of the dispersion curve of these PCFs to variations in the transverse scale is approximately the same (and close to that for the HH PCF). However, in the case of variations in the diameter d_1 of the first-row holes, the HT1 PCF proved to be considerably more stable than the HH1 PCF, the shift of the dispersion zero for the former being half that for the latter. It is obviously explained by the stabilising effect of air gaps between tubes in the HT1 PCF.

The HH1 and HT1 PCFs have approximately identical effective areas of the fundamental mode, the dispersion curve slopes, and numerical apertures. The latter proved to be the lowest among the numerical apertures of fibres studied. The HH PCF has the largest numerical aperture.

Note in conclusion that the numerical simulation of tellurite-tungstate $80TeO_2 - 20WO_3$ glass PCFs ($n \approx 2.11$ at a wavelength of 1.5 μm) taking into account the frequency dispersion of the refractive index allows us to propose several variants of structures of such fibres for applications in parametric fibre devices:

(1) The PCF formed by a filled central hole in a simple hexagonal lattice of cylindrical holes in a glass with the distance between the hole centres $\Lambda = 1.50$ μm and the hole diameter $d = 0.78$ μm. This fibre will have the zero dispersion at a wavelength of 1.545 μm with the dispersion slope ~ 0.37 ps nm^{-2} km^{-1}, it will be single-mode for wavelengths $\lambda \gtrsim 1.1$ μm, and will have the effective area of ther fundamental mode $A_{\text{eff}} \approx 3.0$ μm^2 and the numerical aperture NA ≈ 0.60 at the operating wavelength 1.55 μm.

(2) The PCF formed by a filled central hole in a simple square lattice of cylindrical holes in a glass with the distance between the hole centres $\Lambda = 1.20$ μm and the hole diameter $d = 0.64$ μm. This fibre will have the zero dispersion at a wavelength of 1.551 μm with the dispersion slope ~ 0.28 ps nm^{-2} km^{-1}, it will be single-mode at wavelengths

$\lambda \gtrsim 0.9$ μm and will have the effective area of the fundamental mode $A_{\text{eff}} \approx 2.5$ μm^2 and the numerical aperture NA ≈ 0.41 at the operating wavelength.

(3) PCFs formed by a filled central hole in a simple hexagonal lattice of cylindrical holes in a glass with the distance between the hole centres $\Lambda = 2.20$ μm, the diameter of the first-row holes around the filled hole $d_1 = 1.76$ μm and the diameter of the rest of the holes in the range 1.1 μm $\lesssim d \lesssim$ 1.5 μm. For holes of any diameter within this range, such fibres will have the zero dispersion at a wavelength of 1.542 μm with the dispersion slope ~ 0.40 ps nm^{-2} km^{-1}, the effective area of the fundamental mode $A_{\text{eff}} \approx 3.6$ μm^2, the numerical aperture $NA \approx 0.41$ at the operating wavelength 1.55 μm, and will be single-mode at wavelengths $\lambda \gtrsim 1.0$ μm.

(4) PCFs formed by a filled tube in a simple hexagonal lattice of cylindrical glass tubes with the distance between their centres (external diameter) $\Lambda = D = 2.70$ μm, the internal diameter of the first-row tubes around the filled tube $d_1 = 2.16$ μm and the internal diameter of the rest of the holes in the range 0.25 μm $\lesssim d \lesssim 0.80$ μm. For tubes of any internal diameter within this range, such fibres will have the zero dispersion at a wavelength of 1.548 μm with the dispersion slope ~ 0.40 ps nm^{-2} km^{-1}, the effective area of the fundamental mode $A_{\text{eff}} \approx 3.3$ μm^2, the numerical aperture $NA \approx 0.42$ at the operating wavelength 1.55 μm, and will be single-mode at wavelengths $\lambda \gtrsim 0.8$ μm.

References

1. Birks T.A., Knight J.C., Russell P.St.J. *Opt. Lett.*, **22**, 961 (1997).
2. Mogilevtsev D., Birks T.A., Russell P.St.J. *Opt. Lett.*, **23**, 1662 (1998).
3. Bennett P.J., Monro T.M., Richardson D.J. *Opt. Lett.*, **24**, 1203 (1999).
4. Broderick N.G.R., Monro T.M., Bennett P.J., Richardson D.J. *Opt. Lett.*, **24**, 1395 (1999).
5. Ferrando A., Silvestre E., Moret J.J., Andrés P. *Opt. Lett.*, **25**, 790 (2000).
6. Knight J.C., Birks T.A., Gregan R.F., Russell P.St.J., de Sandro J.-P. *Electron. Lett.*, **13**, 1347 (1998).
7. Biryukov A.S., Dianov E.M., in *Volokonno-opticheskie tekhnologii, materially i ustroistva* (Fibreoptic Technologies, Materials, and Devices) (Kaluga; Izd. N. Bochkarevoi, 2002) No 5, p. 6.
8. Eberly J.H. *Opt. Expr.*, **9**, 674 (2001).
9. El-Mallawany R.A.H. *Tellurite Glasses Handbook* (New York: CRC Press, 2002).
10. Stegeman R., Jankovic L., Kim H., Rivero C., Stegeman G., Richardson K., Delfyett P., Guo Y., Schulte A., Cardinal T. *Opt. Lett.*, **28**, 1126 (2003).
11. Hu E.S., Hsueh Y.-L., Marhic M.E., Kazovsky L.G. *Proc. 28th Europ. Conf. Opt. Communi.* (Copenhagen, Denmark, 2002) Paper 3.2.3.
12. Mori A., Shikano K., Enbutsu K., Oikawa K., Naganuma K., Kato M., Aozasa S. *Proc. 30th Europ. Conf. Opt. Commun.* (Stockholm, Sweden, 2004) Paper 3.3.6.
13. Ghosh G. *J. American Ceramical Society*, **78**, 2828 (1995).
14. Mortensen N.A. *Opt. Express*, **10**, 341 (2002).
15. Mortensen N.A., Folkenberg J.R., Skovgaard P.M.W., Broeng J. *IEEE Photon. Technol. Lett.*, **14**, 1094 (2002).
16. Johnson S.G., Joannopoulos J.D. *Opt. Express*, **8**, 173 (2001).
17. Johnson S.G. *The MIT Photonic-Bands. Manual* (Cambrige: Massachusetts Institute of Technology, 2003).